Feasibility of Single-Time-Point Dosimetry for Radiopharmaceutical Therapies

Xinchi Hou[1], Julia Brosch[2], Carlos Uribe[1,3], Alessandro Desy[4,5], Guido Böning[2], Jean-Mathieu Beauregard[4,5], Anna Celler[1], and Arman Rahmim[1,3,6]

[1]*Department of Radiology, University of British Columbia, Vancouver, British Columbia, Canada;* [2]*Department of Nuclear Medicine, University Hospital, Ludwig-Maximilians-Universität, Munich, Germany;* [3]*Functional Imaging, BC Cancer, Vancouver, British Columbia, Canada;* [4]*Cancer Research Centre and Department of Radiology and Nuclear Medicine, Université Laval, Quebec City, Quebec, Canada;* [5]*Department of Medical Imaging and Oncology, Université Laval Research Centre, CHU de Québec–Université Laval, Quebec City, Quebec, Canada; and* [6]*Department of Integrative Oncology, BC Cancer Research Institute, Vancouver, British Columbia, Canada*

Because of challenges in performing routine personalized dosimetry in radiopharmaceutical therapies, interest in single-time-point (STP) dosimetry, particularly using only a single SPECT scan, is on the rise. Meanwhile, there are questions about the reliability of STP dosimetry, with limited independent validations. In the present work, we analyzed 2 STP dosimetry methods and evaluated dose errors for several radiopharmaceuticals based on effective half-life distributions. **Methods:** We first challenged the common assumption that radiopharmaceutical effective half-lives across the population are gaussian-distributed (i.e., follow a normal distribution). Then, dose accuracy was estimated using 2 STP dosimetry methods for a wide range of potential post injection (p.i.) scan time points for different radiopharmaceuticals applied to neuroendocrine tumors and prostate cancer. The accuracy and limitations of each of the STP methods were discussed. **Results:** A lognormal distribution was more appropriate for capturing effective half-life distributions. The STP framework was promising for dosimetry of ^{177}Lu-DOTATATE and for kidney dosimetry of different radiopharmaceuticals (errors $< 30\%$). Meanwhile, for some radiopharmaceuticals, STP accuracy was compromised (e.g., in bone marrow and tumors for ^{177}-labeled prostate-specific membrane antigen [PSMA]). The optimal SPECT scanning time for ^{177}Lu-DOTATATE was approximately 72 h p.i., whereas 48 h p.i. was better for ^{177}Lu-PSMA. **Conclusion:** Simplified STP dosimetry methods may compromise the accuracy of dose estimates, with some exceptions, such as for ^{177}Lu-DOTATATE and for kidney dosimetry in different radiopharmaceuticals. Simplified personalized dosimetry in the clinic continues to be challenging. On the basis of our results, we make suggestions and recommendations for improved personalized dosimetry using simplified imaging schemes.

Key Words: dosimetry; quantitation; radiopharmaceutical therapy; SPECT; single-time-point

J Nucl Med 2021; 62:1006–1011
DOI: 10.2967/jnumed.120.254656

Image-based personalized dosimetry as applied to radiopharmaceutical therapies allows physicians to limit toxicity to critical organs and, potentially, to predict response to treatment and enable personalized therapy decisions (*1*). To perform dosimetry with acceptable accuracy, multiple quantitative scans (e.g., SPECT) are often assumed necessary to assess the distribution of the therapeutic compound over time and quantify its biokinetics in organs and tumors. Nevertheless, this task is challenging in a clinical environment because of the requirement that a series of scans be performed over multiple days for each therapy cycle in each patient, followed by complex and time-consuming data processing and calculations (*2*).

To address this challenge, with the aim of enabling routine dosimetry in the clinic, several simplified approaches have been proposed. One approach is to perform dosimetry estimation using only a single SPECT scan (single-time-point [STP] dosimetry) (*3–8*).

STP methods have been proposed by Hänscheid et al. (*3*) and Madsen et al. (*4*). Both methods assume that clearance of the radiopharmaceutical from a region of interest (ROI) follows a monoexponential decay behavior and has an effective half-life (T_{eff}); therefore, the time-integrated activity $\tilde{A}$ in the ROI can be calculated using the following formula:

$$\tilde{A} = \frac{1}{ln2} \cdot A(T_{sc}) \cdot 2^{\frac{T_{sc}}{T_{eff}}} \cdot T_{eff}, \qquad \text{Eq. 1}$$

where T_{sc} is the SPECT scan time point and $A(T_{sc})$ is activity in the ROI measured at T_{sc}. This activity can be determined from the quantitatively reconstructed SPECT image. However, T_{eff} may be difficult to measure, requiring a series of SPECT scans with subsequent data fitting for the ROIs. Furthermore, T_{eff} can vary significantly between individual patients and/or between therapy cycles.

The STP method of Hänscheid et al. (*3*) proposes that the last component of Equation 1, that is, $2^{\frac{T_{sc}}{T_{eff}}} \cdot T_{eff}$, can be approximated by $2T_{sc}$. Their theoretic calculations indicated that if T_{sc} remains within 0.75–2.5 times the patient-specific T_{eff}, errors in dose estimates would be below 10%. Hänscheid et al. analyzed 29 ^{177}Lu-DOTATATE/DOTATOC patient studies to confirm this theoretic finding (*3*).

On the other hand, the work published by Madsen et al. (*4*), based on ^{90}Y-DOTATOC data from a clinical trial, used a population mean T_{eff} ($T_{p\text{-}eff}$) and demonstrated that the accuracy of STP dosimetry for kidneys would be improved by setting T_{sc} close to or slightly larger than $T_{p\text{-}eff}$ (*4*). This STP dosimetry framework was verified to have good accuracy by Amato et al. in the treatment of hyperthyroidism with ^{131}I radioiodine (*9*). Both formulations—that of Hänscheid et al.

Received Aug. 5, 2020; revision accepted Oct. 8, 2020.
For correspondence or reprints, contact Xinchi Hou (arman.rahmim@ubc.ca).
Published online Oct. 30, 2020.

(method 1) and that of Madsen et al. (method 2)—are presented in Table 1.

Inspired by these works, we recently investigated the accuracy of STP dosimetry for kidneys using different values of T_{sc} (4, 24, and 72 h p.i.) for data from 53 neuroendocrine tumors in 39 patients undergoing ^{177}Lu-DOTATATE therapy (*6*). The impact of the deviation of a particular T_{eff} from $T_{p\text{-}eff}$ on the accuracy of kidney doses was estimated. The most favorable T_{sc}, that is, the scan that would result in kidney dosimetry errors below 10%, was suggested to be set at times between 1 and 1.5 $T_{p\text{-}eff}$. However, our previous study was focused solely on kidney doses and on a single specific compound, namely ^{177}Lu-DOTATATE.

For a given patient, the T_{eff} for radiopharmaceutical clearance from tumors usually differs from that from organs at risk (OARs). Compromise is needed to achieve acceptably accurate dose estimates using STP methods, as the optimal T_{sc} for tumors may be different from that for OARs. These time points would also differ for different radiopharmaceutical compounds.

In the present work, we compared the accuracy of doses estimates using STP methods 1 and 2 for different compounds commonly applied in radiopharmaceutical therapies. We also challenged the common default assumption that T_{eff} has a gaussian (normal) distribution across a population. On the basis of our results, we provide recommendations for dosimetry workflows.

MATERIALS AND METHODS

Because the mean organ-based absorbed dose can be considered nearly proportional to $\tilde{A}$, the dose error (DE) can be estimated from the time-integrated activities (as estimated using either method 1 or 2) as follows:

$$\mathrm{DE}\ (\%) = \left(\frac{\tilde{A}_{Mx}}{\tilde{A}} - 1\right) \times 100\%, \qquad \text{Eq. 2}$$

where $\tilde{A}_{Mx}$ represents either $\tilde{A}$ for either method 1 or method 2 (Table 1), and reference $\tilde{A}$ is calculated using Equation 1. We investigated T_{sc} ranging from 24 to 144 h (days 1–6) after activity injection.

Using these T_{sc} values, we estimated DEs for generic patient-specific T_{eff} values ranging from 0 to 200 h. Whereas method 1 does not depend on T_{eff}, for method 2 $T_{p\text{-}eff}$ was set between 10 and 120 h to capture a wide range of possibilities. Subsequently, for both tumors and OARs, DEs were investigated using these 2 STP methods for 4 commonly applied radiopharmaceuticals, namely ^{177}Lu-DOTATATE and ^{90}Y-DOTATOC, as used in treatments of neuroendocrine tumors, and ^{177}Lu-labeled prostate-specific membrane antigen (PSMA) compounds (including ^{177}Lu-PSMA-617 and ^{177}Lu-PSMA-I&T), as used for prostate cancer.

To investigate the accuracy of STP dosimetry, we aimed to first obtain 95% confidence intervals (CIs) for the distributions of T_{eff} for a given radiopharmaceutical and organ or target of interest. Table 2 summarizes T_{eff} for different radiopharmaceuticals as available in the literature or from our own data. For most datasets, limited information, such as mean, standard deviation (SD) and ranges for T_{eff}, could be found, with the exception of 5 datasets from our own clinical studies (i.e., studies 1, 4 and 8 in Table 2, for which the individual T_{eff} values for patients were available). For studies 1 and 4, patient data were from the radiopharmaceutical therapy trial NCT02754297, approved by the CHU de Québec–Université Laval institutional Ethics Committee, and all patients provided written consent to participate. Study 8 was based on retrospective and anonymized data, acquired for routine clinical dosimetry, as approved by the Ethics Committee of LMU Munich 20-520, including a waiver of consent.

On the basis of a common default assumption that T_{eff} follows a normal distribution, 95% CIs would be set at mean ± 1.96 SD. By contrast, our analysis in this work showed that a lognormal distribution is a more proper assumption. For each of our 5 full datasets with a complete listing of T_{eff} values (studies 1, 4, and 8 in Table 2), the Kolmogorov–Smirnov test was performed to check the null hypothesis that our data or their corresponding log-transformation were normally distributed. Furthermore, distribution fittings were performed and analytic 95% CIs for the T_{eff} per ROI were calculated and compared with the true range of 95% CI data as calculated using the quantile function. Having found that a lognormal distribution is a more appropriate model, we mapped the reported means and SDs from different studies to lognormal distributions with exponent parameters μ and σ (i.e., mean and SD of the natural logarithm) as given in the following equations:

$$\mu = \log\left(\frac{\mathrm{mean}^2}{\sqrt{\mathrm{mean}^2 + \mathrm{SD}^2}}\right) \qquad \text{Eq. 3}$$

$$\sigma = \sqrt{\log(1 + \mathrm{SD}^2/\mathrm{mean}^2)}\ . \qquad \text{Eq. 4}$$

Subsequently, from the mapped lognormal distributions, 95% CI ranges were computed. Finally, DEs for the computed ranges (spreads) of T_{eff} were estimated using both method 1 and method 2.

RESULTS

DEs calculated using methods 1 and 2 are presented in Figure 1 for a wide range of $T_{p\text{-}eff}$ and T_{eff}. The DEs within ±10% are highlighted in green. Overall, for both STP methods, the accuracy of dose estimates strongly depended on the spread of patient T_{eff} values and the scan time selected by the users.

The T_{eff} distributions were then investigated using the 5 datasets that had a complete listing of T_{eff} values for ^{177}Lu-DOTATATE and ^{177}Lu-PSMA-I&T (studies 1, 4, and 8). Supplemental Table 1 lists the Kolmogorov–Smirnov test results and p-values, demonstrating that most T_{eff} data followed a lognormal distribution (supplemental materials are available at http://jnm.snmjournals.org). Supplemental Figure 1 shows the corresponding histograms with probability density function curves of lognormal distribution fittings, as well as the true and analytically estimated 95% CI ranges based on normal and lognormal distribution assumptions. Supplemental Figure 2 shows the DEs from these 3 different types of ranges

TABLE 1
STP Dosimetry Application Methods

Method	Approximation	Conclusion
1 (*3*)	$\tilde{A} = \frac{1}{\ln 2} \cdot A(T_{sc}) \cdot 2\ T_{sc}$	Error $< 10\%$ if $T_{sc} \in [0.75T_{eff}, 2.5T_{eff}]$
2 (*4*,*7*)	$\tilde{A} = \frac{1}{\ln 2} \cdot A(T_{sc}) \cdot 2^{\frac{T_{sc}}{T_{p-eff}}} \cdot T_{p-eff}$	Smallest errors can be observed if $T_{sc} \in [T_{p-eff}, 1.5T_{p-eff}]$

TABLE 2
Mean T_{eff} and SD, and Computed 95% CI, of Organs and Lesions for Commonly Applied Radiopharmaceuticals That Were Used in This Investigation

Agent	Study	Reference	Patients (*n*)	Organ or target	Median	T_{p-eff} mean (h)	T_{p-eff} SD (h)	95% CI (h)
^{177}Lu-DOTATATE	1	Hou et al. 2019 (*12*)	30 (87)	Kidney*	46 (30–82)	47.0	11.6	28.5–73.6
	2	Heikkonen et al. 2016 (*13*)	24 (24)	Kidney	NA (36–59)	45.3	5.9	34.8–57.4
	3	Hänscheid et al. 2018 (*3*)†	27 (54)	Kidney‡	51 (40–68)	51.0	7.0	38.8–66.0
			25 (25)	Liver‡	67 (55–117)	76.5	15.5	51.4–110.7
			27 (27)	Spleen‡	68 (52–99)	68.0	11.8	49.5–91.6
			22 (22)	Tumor‡	77 (56–130)	85.4	18.5	56.0–125.8
	4	Del Prete et al. 2018 (*11*)	158 (1,117)	Kidney* ‡	47 (23–159)	50.8	16.9	25.6–91.0
		Desy et al. *2020* (*14*)	158 (474)	Bone marrow* ‡	70 (29–160)	76.4	27.6	36.2–142.8
			158 (2,166)	Tumor* ‡	84 (16–161)	87.8	30.5	42.8–160.6
^{90}Y-DOTATOC	5	Menda et al. 2018 (*15*)	25 (69)	Kidney	NA (25–92)	37.5	12.5	19.4–67.2
^{177}Lu-PSMA-617	6	Kurth et al. 2018 (*16*)	25 (25)	Whole body	NA (22–86)	40.5	15.8	18.8–79.1
	7	Sarnelli et al. 2019 (*17*)	9 (9)	Parotid gland	33 (26–61)	35.4	10.6	22.2–53.2
			9 (9)	Kidney	31 (12–81)	39.2	20.9	17.2–76.2
			9 (9)	Red marrow	8 (3–15)	8.0	4.7	3.2–16.3
			9 (9)	Liver	25 (13–63)	33.5	20.0	13.4–69.1
			9 (9)	Whole body	40 (32–80)	52.4	22.2	27.2–90.5
^{177}Lu-PSMA-I&T	8	Written communications	15 (290)	Bone metastases*	38 (13–191)	42.6	19.1	16.9–90.0
	9	Baum et al. 2016 (*18*)	30 (NA)	Bone metastases‡	52 (14–149)	52.0	30.0	16.2–132.6
			30 (NA)	Lymph nodemetastases‡	43 (25–160)	43.0	32.0	9.9–132.7
			30 (NA)	Kidney‡	33 (19–83)	33.0	14.0	14.8–64.9
			30 (NA)	Parotid gland‡	25 (20–43)	25.0	5.0	16.7–36.1

*T_{eff} of each individual ROI (organ or lesion) was available (i.e., complete listing of T_{eff} for all patients).
†Overall dataset (29 patients) was primarily ^{177}Lu-DOTATATE (22 patients) but also included ^{177}Lu-DOTATOC (7 patients).
‡T_{eff} was published as median and range. For studies 3 and 9, corresponding mean and SD were calculated using method of Hozo et al. 2005 (*19*). For study 4, we had access to complete listing of T_{eff}.
NA = not applicable.
Data in parentheses are range (for median) or total number of ROIs (for number of patients).

(i.e., computed on the basis of the true 95% CI vs. normal and lognormal assumptions), confirming that doses computed from a lognormal distribution were more similar to those from the true 95% CI range, further strengthening the lognormal assumption.

Table 2 shows our computed 95% CI ranges based on a lognormal distribution assumption, using the means and SDs reported in the literature. Had we assumed a normal distribution, the computed 95% CIs of T_{eff} would extend below 0 for some studies. Based on these T_{eff}, the DEs for the investigated radiopharmaceuticals are presented in Figures 2 and 3 for kidney and bone marrow, respectively, which are OARs for the particular radiopharmaceutical therapies investigated, and in Figure 4 for tumors. For ^{177}Lu-DOTATATE, the estimated DEs were relatively low, whereas for some other radiotracers, large errors were possible for both STP dosimetry methods. Additionally, a comparison between the DEs for the published range listed in Table 2 and those for the estimated 95% CI is shown in Supplemental Figure 3.

DISCUSSION

As shown in Figure 1, when T_{sc} ranged from 0.8 to 1.6 $T_{p\text{-}eff}$, the DEs from both method 1 and method 2 were similar (differences < 7%). DE was small (<10%) when T_{sc} was set within 0.75–2.5 T_{eff} for method 1, as is consistent with prior reporting (*3*). However, for method 2, the accuracy of absorbed dose depended not only on T_{sc} but also on the deviation of T_{eff} from $T_{p\text{-}eff}$. Overall, T_{sc} should preferably be set in the range 1–1.5 $T_{p\text{-}eff}$ in order to achieve a lower DE but allow larger deviations between T_{eff} and $T_{p\text{-}eff}$. This recommendation agrees with Figure 4 of Zhao et al. (*6*). For example, if $T_{p\text{-}eff}$ was 47 h (the kidney's $T_{p\text{-}eff}$ for ^{177}Lu-DOTATATE in study 1; Table 2) and T_{sc} was set to 72 h, less than a 10% DE could be observed when the deviation between $T_{p\text{-}eff}$ and T_{eff} was within a 95% CI of −38% to 43% if T_{sc} was set to 72 h. However, when T_{sc} was set to 24 h p.i., the deviation between $T_{p\text{-}eff}$ and T_{eff} had to stay within a 95% CI of −10% to 10% in order to have a DE of less than 10%.

Figures 2–4 summarize potential DEs based on the analysis of our own or published T_{eff} values for commonly used radiopharmaceuticals. In general, our results suggest that there is a high possibility of dose underestimation when using an STP framework. The extent of this underestimation would depend on the radiopharmaceutical and the considered ROI, particularly the kidneys, the bone marrow, and neuroendocrine tumors.

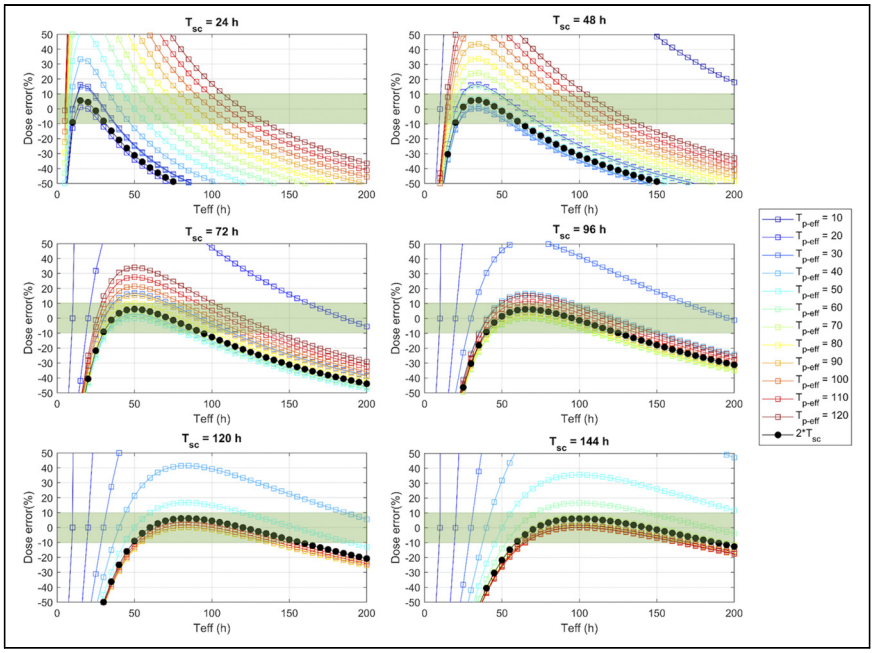

FIGURE 1. DEs (%) resulting from method 1 (black line) and method 2 (with $T_{p\text{-}eff}$ ranging from 10 to 120 h; colored lines) relative to true T_{eff} of radiopharmaceutical washout. DEs within ±10% are highlighted in green.

For the kidneys, similar DEs were obtained from both method 1 and method 2 when T_{sc} was set to 48–96 h (i.e., days 2–4 p.i.), as shown in Figure 2. However, large differences between methods 1 and 2 were observed for either an early T_{sc} (24 h p.i.) or a late T_{sc} (>96 h p.i.). For most of the investigated radiopharmaceuticals, DEs were smallest when T_{sc} was set to 48 h p.i. However, for ^{177}Lu-DOTATATE, a T_{sc} of 72 h p.i. was slightly better than a T_{sc} of 48 h p.i., with a DE of less than 10%. For ^{177}Lu-PSMA-compound therapies, DE could be larger than 20% even at an optimized T_{sc}.

For bone marrow dosimetry (Fig. 3), DEs were smallest (<30%) when T_{sc} was set to 72–96 h p.i. for ^{177}Lu-DOTATATE. However, for ^{177}Lu-PSMA-617, STP methods should be used only with great caution, because in most of our investigated scenarios, STP methods largely underestimated the dose, especially method 1.

For neuroendocrine tumor lesions treated with ^{177}Lu-DOTATATE (Fig. 4), similar to bone marrow dosimetry, a T_{sc} of 72–120 h p.i. resulted in a DE of less than 30%, whereas for prostate cancer lesions treated with ^{177}Lu-PSMA-I&T, DEs (<30%) were lowest for a T_{sc} of 48 h p.i., as displayed in Figure 4.

Additionally, differences in DEs for the same radiopharmaceutical and ROI were found between different studies, mainly because of differences in the methods used to estimate T_{eff} by different groups, including segmentation method, imaging type, and T_{sc}, as well as fitting model. For example, the analysis in study 1 was based on small-volume kidney dosimetry, using a 4 -mL region within the kidney for dose estimation, whereas for study 2, the data were from whole-kidney segmentation. As another example, study 8 used 3 SPECT/CT scans, whereas 5 hybrid SPECT/planar scans were used in study 9. However, these differences did not influence our main findings in this work.

The STP dosimetry framework is suitable mostly for dosimetry of ^{177}Lu-DOTATATE and of various radiopharmaceuticals in kidneys.

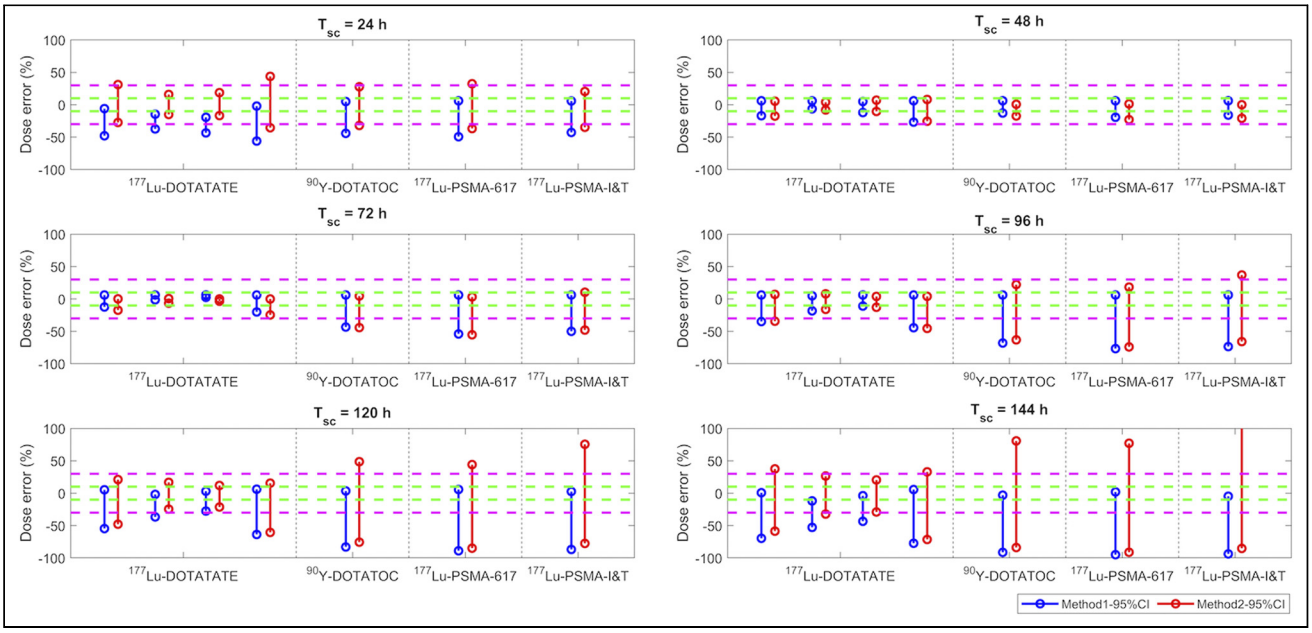

FIGURE 2. DEs (%) of kidney doses estimated using method 1 (blue) and method 2 (red) when patient T_{eff} is within simulated 95% CI range listed in Table 2. Green and magenta dashed lines indicate ±10% and ±30% of DEs, respectively. Four sets of results shown in ^{177}Lu-DOTATATE column correspond to T_{eff} data from studies 1–4.

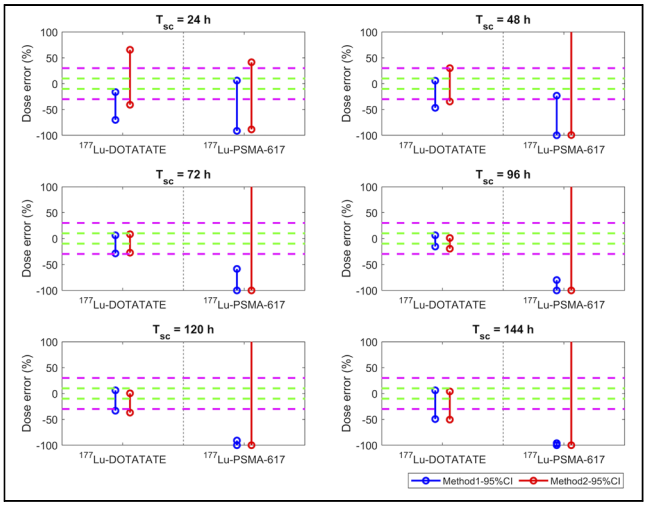

FIGURE 3. DEs (%) of bone marrow doses estimated using method 1 (blue) and method 2 (red) when patient T_{eff} is within simulated 95% CI range from Table 2. Green and magenta dashed lines indicate ±10% and ±30% of DEs, respectively. Two sets of results correspond to data from studies 4 and 7.

Our results were less reliable for ^{177}Lu-PSMA compounds in bone marrow and lesions. If the results for kidneys, bone marrow, and tumors are combined, SPECT scanning at 72 h p.i. should be considered optimal for ^{177}Lu-DOTATATE whereas earlier time points, such as 48 h p.i., would be better for ^{177}Lu-PSMA therapies, in agreement with findings by Zhao et al. and Jackson et al. (*6*,*7*). The results for methods 1 and 2 were equally accurate when the suggested scan time was used.

The potentially large differences in pharmaceutical clearance rate between patients, and the limited data available for our analysis, suggest that the DEs obtained from STP methods could be 30% or more for some therapeutic compounds and targets. More studies or potential modifications of the STP methods are needed. For example, Jackson et al. (*7*) applied an STP method to predict doses from ^{177}Lu-PSMA-617 therapy using a population of normalized pharmacokinetic curves. However, the accuracy of that method has not been confirmed, and accuracy was represented by the mean absolute error, which could be smaller than the DE format we report here (*8*). In addition, individual clinical data might be used to narrow the range of T_{eff} around which STP scans could be performed. As an example, we suggest that variations in estimated glomerular filtration rate (eGFR) may indicate varying kidney function, in turn impacting T_{eff}. In fact, we investigated and found a significant correlation between these 2 factors (Supplemental Fig. 4). A similar correlation between kidney dose and eGFR was also found by Del Prete et al. in 2017 (*10*). Thus, a potentially improved STP framework would use a modified estimated T_{eff} based on such clinical parameters.

Our results show that the accuracy of STP framework depends strongly on patient-specific radiopharmaceutical clearance times, and the large differences between patients suggest that STP methods may not be appropriate for all therapies or radiopharmaceuticals. When STP may be problematic, an alternative practical approach for patient-specific dosimetry may be to use at least 2 time points for imaging and subsequent T_{eff} calculation for the first cycle of treatment to estimate patient-specific pharmaceutical kinetics, specifically patient- and organ-specific T_{eff} . However, the choice of T_{sc} for the 2 scans is crucial, and one should avoid setting them during the early radiopharmaceutical uptake phase. Afterward, this information could be incorporated into the more generalized form (Eq. 1) to estimate T_{eff} for the following cycles. The accuracy of such an approach was investigated by Del Prete et al. (*11*), who observed DEs of approximately −0.5%, 15.7%, and −5.6% for kidney, bone marrow, and tumor, respectively, for ^{177}Lu-DOTATATE.

CONCLUSION

We have analyzed the accuracy of 2 STP dosimetry methods for several radiopharmaceutical therapy agents. We found that for some therapeutic compounds, use of these simplified methods may largely compromise the accuracy of dose estimates. Two prominent exceptions are ^{177}Lu-DOTATATE, wherein reasonably small (<30%) DEs can be achieved for an STP framework that scans at approximately 72 h p.i., and kidney dosimetry in general for radiopharmaceuticals investigated in this work. To improve STP dosimetry, we suggest the alternative approach of determining patient-specific biokinetics using 2 or, ideally, more scans during the first treatment cycle and the STP framework for the following cycles. However, this approach needs to be validated, since T_{eff} might change over multiple treatment cycles. Other alternatives to existing STP methods include improved estimation of patient-specific T_{eff} from clinical data, as exemplified in this work using eGFRs for the kidney. Enabling routine personalized dosimetry in the clinic remains challenging given the complex data processing and calculations for high accuracy on the one hand and interest in more feasible methods on the other.

DISCLOSURE

This work was supported by grant 137993 from the National Institutes of Health/Canadian Institutes of Health Research (CIHR) Quantitative Imaging Network, by the German Research Foundation within Research Training Group GRK2274, by a clinical research scholarship from the Fonds de recherche du Québec–Santé, and by

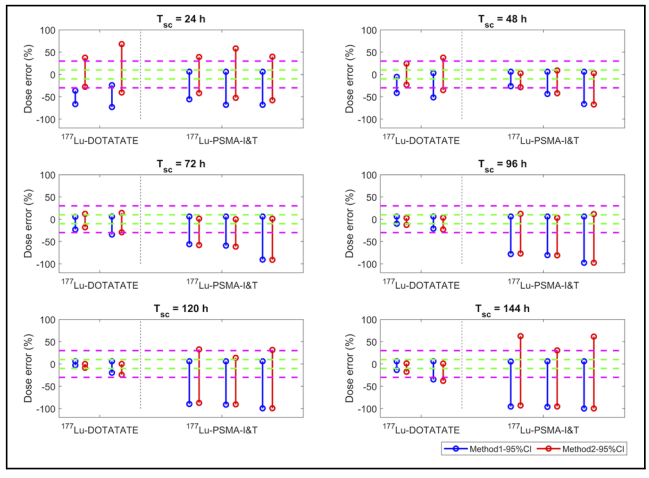

FIGURE 4. DEs (%) of tumor doses estimated using method 1 (blue) and method 2 (red) when patient T_{eff} is within 95% CI range from Table 2. Green and magenta dashed lines indicate ±10% and ±30% of DEs, respectively. Data in ^{177}Lu-DOTATATE column correspond to studies 3 and 4, whereas data in ^{177}Lu-PSMA-I&T column correspond to bone and lymph node metastasis data from studies 8 and 9.

CIHR operating grant MOP-142233. No other potential conflict of interest relevant to this article was reported.

KEY POINTS

QUESTION: Is STP dosimetry feasible in current clinical studies for all radiopharmaceutical therapies?

PERTINENT FINDINGS: The accuracy of STP dose estimation was compromised for some radiopharmaceuticals—for example, ^{177}Lu-PSMA compounds in bone marrow and bone lesions.

IMPLICATIONS FOR PATIENT CARE: We suggest caution and provide guidance for the use of simplified dosimetry protocols in clinical radiopharmaceutical therapy.

REFERENCES

1. Stabin MG, Madsen MT, Zaidi H. Personalized dosimetry is a must for appropriate molecular radiotherapy. *Med Phys*. 2019;46:4713–4716.
2. Ljungberg M, Gleisner KS. Personalized dosimetry for radionuclide therapy using molecular imaging tools. *Biomedicines*. 2016;4:1–21.
3. Hänscheid H, Lapa C, Buck AK, Lassmann M, Werner RA. Dose mapping after endoradiotherapy with ^{177}Lu-DOTATATE/DOTATOC by a single measurement after 4 days. *J Nucl Med*. 2018;59:75–81.
4. Madsen MT, Menda Y, O'Dorisio TM, O'Dorisio MS. Technical note: single time point dose estimate for exponential clearance. *Med Phys*. 2018;45:2318–2324.
5. Willowson KP, Eslick E, Ryu H, Poon A, Bernard EJ, Bailey DL. Feasibility and accuracy of single time point imaging for renal dosimetry following ^{177}Lu-DOTATATE ('Lutate') therapy. *EJNMMI Phys*. 2018;5:33.
6. Zhao W, Esquinas PL, Frezza A, Hou X, Beauregard JM, Celler A. Accuracy of kidney dosimetry performed using simplified time activity curve modelling methods: a ^{177}Lu-DOTATATE patient study. *Phys Med Biol*. 2019;64:175006.
7. Jackson PA, Hofman MS, Hicks RJ, Scalzo M, Violet J. Radiation dosimetry in ^{177}Lu-PSMA-617 therapy using a single posttreatment SPECT/CT scan: a novel methodology to generate time- and tissue-specific dose factors. *J Nucl Med*. 2020; 61:1030–1036.
8. Hänscheid H, Lassmann M. Will SPECT/CT cameras soon be able to display absorbed doses? Dosimetry from single activity concentration measurements. *J Nucl Med*. 2020;61:1028–1029.
9. Amato E, Campennì A, Ruggeri RM, Auditore L, Baldari S. Comment on: "technical note: single time point dose estimate for exponential clearance. *Med Phys* [Med. Phys. 45(5), 2318-2324 (2018)]. 2019;46:2776–2779.
10. Del Prete M, Buteau FA, Beauregard JM. Personalized ^{177}Lu-octreotate peptide receptor radionuclide therapy of neuroendocrine tumours: a simulation study. *Eur J Nucl Med Mol Imaging*. 2017;44:1490–1500.
11. Del Prete M, Arsenault F, Saighi Net al. Accuracy and reproducibility of simplified QSPECT dosimetry for personalized ^{177}Lu-octreotate PRRT. *EJNMMI Phys*. 2018;5:25.
12. Hou X, Zhao W, Beauregard JM, Celler A. Personalized kidney dosimetry in ^{177}Lu-octreotate treatment of neuroendocrine tumours: a comparison of kidney dosimetry estimates based on a whole organ and small volume segmentations. *Phys Med Biol*. 2019;64:175004.
13. Heikkonen J, Mäenpää H, Hippeläinen E, Reijonen V, Tenhunen M. Effect of calculation method on kidney dosimetry in ^{177}Lu-octreotate treatment. *Acta Oncol*. 2016; 55:1069–1076.
14. Desy A, Bouvet GF, Frezza A, Després P, Beauregard JM. Impact of dead time on quantitative ^{177}Lu-SPECT (QSPECT) and kidney dosimetry during PRRT. *EJNMMI Phys*. 2020;7:32.
15. Menda Y, Madsen MT, O'Dorisio TMet al. ^{90}Y-DOTATOC dosimetry-based personalized peptide receptor radionuclide therapy. *J Nucl Med*. 2018;59:1692–1698.
16. Kurth J, Krause BJ, Schwarzenböck SM, Stegger L, Schäfers M, Rahbar K. External radiation exposure, excretion, and effective half-life in ^{177}Lu-PSMA-targeted therapies. *EJNMMI Res*. 2018;8:32.
17. Sarnelli A, Belli ML, Di Iorio Vet al. Dosimetry of ^{177}Lu-PSMA-617 after mannitol infusion and glutamate tablet administration: preliminary results of EUDRACT/RSO 2016-002732-32 IRST protocol. *Molecules*. 2019;24:621.
18. Baum RP, Kulkarni HR, Schuchardt Cet al. ^{177}Lu-labeled prostate-specific membrane antigen radioligand therapy of metastatic castration-resistant prostate cancer: safety and efficacy. *J Nucl Med*. 2016;57:1006–1013.
19. Hozo SP, Djulbegovic B, Hozo I. Estimating the mean and variance from the median, range, and the size of a sample. *BMC Med Res Methodol*. 2005;5:13.